CrossMark

ORIGINAL ARTICLE

The presence of stem cells in potential stem cell niches of the intervertebral disc region: an in vitro study on rats

Rui Shi[1] · Feng Wang[1] · Xin Hong[1] · Yun-Tao Wang[1] · Jun-Ping Bao[1] ·
Feng Cai[1] · Xiao-Tao Wu[1]

Abstract

Purpose   The potential of stem cell niches (SCNs) in the intervertebral disc (IVD) region, which may be of great significance in the regeneration process, was recently proposed. To the best of our knowledge, no previous in vitro study has examined the characteristics of stem cells derived from the potential SCN of IVD (ISN). Therefore, increasing knowledge on ISN-derived stem cells (ISN-SCs) may provide a greater understanding of IVD degeneration and regeneration processes. We aimed to demonstrate the existence of ISN-SCs and to compare their characteristics with bone marrow mesenchymal stem cells (BMSCs) in vitro.

Methods   Sprague–Dawley rats (male, 10-week-old) were used in this study. ISN tissues were separated by ophthalmic surgical instruments under a dissecting microscope according to the anatomical areas. BMSCs and cells isolated from the ISN tissues were cultured and expanded in vitro. Passage 4 populations were used for further analysis with respect to colony-forming ability, cellular immunophenotype, cell cycle, stem cell-related gene expression, and proliferation and multipotential differentiation capacities.

Results   In general, both of ISN-SCs and mesenchymal stromal cells (MSCs) met the minimal criteria for the definition of multipotent mesenchymal stromal cells, including adherence to plastic, specific surface antigen expression, and multipotent differentiation potential. Especially, ISN-SCs even showed greater potential of osteogenesis and chondrogenesis. The ISN-SCs also expressed stem cell-related genes that were comparable to those of BMSCs, and had colony-forming and self-renewal abilities.

Conclusions   To the best of our knowledge, this is the first in vitro study aimed towards determining the existence and characteristics of ISN-SCs, which belong to the MSC family and with greater osteogenic and chondrogenic abilities than BMSCs according to our data. This finding may be of great significance for additional studies that investigate the migration of ISN-SCs into the IVD, and may provide a new perspective on different biological approaches for IVD self-regeneration.

Keywords   Intervertebral disc · Stem cell niches · Mesenchymal stem cells · Cell differentiation · Cellular immunophenotype

Introduction

Presently, low back pain (LBP) has evolved into a serious health problem affecting approximately 80 % of the population, resulting in huge medical costs [1]. Among the numerous and complex causes of LBP, lumber intervertebral disc degeneration (IVDD) is believed to be the most crucial and strongly associated with LBP, especially in its unstable stage [2]. In recent years, biological strategies accompanied with biotechnological developments have emerged for various diseases. Cell therapies for IVDD have made significant headway, mainly focusing on stem cell transplantation [3–5]. Bone marrow mesenchymal stem cells (BMSCs) are highly studied stem cells of different origins, including synovium, periosteum, skeletal muscle, and adipose tissues. Our previous studies demonstrated the

R. Shi and F. Wang contributed equally to this article.

✉ Xiao-Tao Wu
wuxiaotao@medmail.com.cn

[1]   Spine Center, Zhongda Hospital, Medical School, Southeast University, 87 Dingjiaqiao, Nanjing 210009, Jiangsu, China

excellent repair efficiency of BMSCs transplanted into rabbit intervertebral discs (IVDs) [6]. Besides, adipose-derived stem cells have also been extensively used for repair of IVDD with the advantage of convenient availability and abundance [7], and even improve the viability of nucleus pulposus cells in degenerated intervertebral discs [8]. However, the defects of stem cell transplantation were also exposed, such as puncture injury and damage in the process of extracting stem cells from the tissues, also, how to promote survival rate and restore matrix of foreign cells in the hostile environment (acidic, hypoxic and poor in nutrients) of degenerating disc remains a challenge.

Another stem cell-based therapeutic strategy is the induction of endogenous stem cell activity. Since the concept of stem cell niches (SCNs) was introduced by Schofield [9], niches in a variety of tissues and organs have come under observation, including those in the respiratory, digestive, and nervous systems, as well as in the skin, bone marrow, heart, adipose tissue, and feto-placental tissue [10]. SCN is defined as a dynamic microenvironment consisting of the extracellular matrix (ECM) and neighboring cells with the ability of regulating the stem cells present within [9–11]. Migration of endogenous stem cells within the niches into adjacent target regions is a crucial process for tissue self-repair. Therefore, the ability to direct and promote the migration of stem cells within the niche represents a promising strategy for self-rehabilitation in stem cell-based therapies and regenerative medicine. For example, cardiac stem cells (CSCs) can be recruited to infarcted myocardial areas. Furthermore, Wang et al. [12] demonstrated that the repair effect is strongly enhanced by facilitating the migration process. This similar promoting migration to repair (PMR) effect has also been observed in many other tissues [13–16]. Until now, stem cells derived from various parts of the IVD such as the nucleus pulposus (NP), annulus fibrosus (AF), and cartilage endplate (CEP) have been isolated and characterized [17–20], whereas little is known about endogenous stem cell migration with respect to difficulties in labeling target stem cells in vivo.

Recently, a potential SCN within the IVD region (ISN), which may be of great significance in IVD regeneration processes, was proposed by Henriksson et al. [21], representing a new strategy for IVD self-repair. The ISN area was defined as the perichondrium region adjacent to the epiphyseal plate (EP) and outer zone of the AF (AFo), where existing slow cycling cells (a feature of stem cells) were detected by means of an established in vivo labeling method using 5-bromo-2-deoxyuridine (BrdU) [21]. This result was confirmed by a series of in vivo studies where the stem cell migration route was defined from the niches to the AF and inner part of the IVD (Fig. 1) [22–24]. As a consequence, ISN-derived stem cells (ISN-SCs) are likely to be involved in self-regenerative attempts in the IVD.
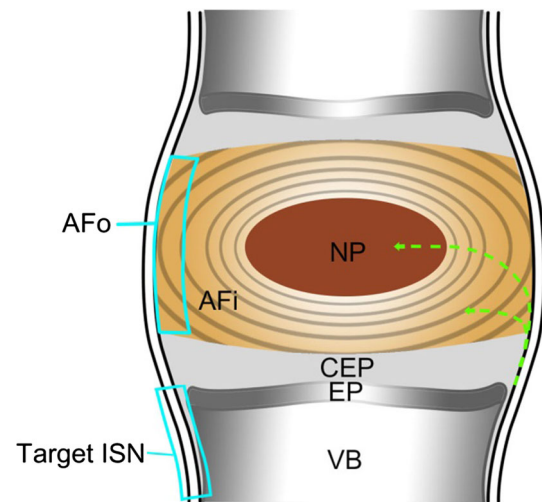

Fig. 1 Schematic graph of the target ISN region and the potential cellular migration pathways (*arrows*). *AFo* outer zone of AF, *AFi* inner part of AF, *NP* nucleus pulposus, *CEP* cartilage endplate, *EP* epiphyseal plate, *VB* vertebral body

This finding of the potential ISN shed new light on biological approaches for IVD self-regeneration, facilitating stem cell migration directly into the IVD. To the best of our knowledge, there has been no report on the isolation and culturing of ISN-SCs in vitro. Moreover, little is known about the characteristics of ISN-SCs, preventing further exploration on the migratory mechanisms and PMR methods in the IVD. To this end, it is meaningful to determine the existence and characteristics of ISN-SCs within the potential ISN using in vitro studies.

In the present study, we isolated and cultured ISN-SCs in vitro and determined the characteristics with regard to colony formation, cellular immunophenotype, cell cycle, stem cell-related gene expression, and proliferation and multipotential differentiation capacities. Rats were chosen as the experimental model since they are commonly used in IVD research [24–26]. Considering that the perichondrium region adjacent to the EP may be the common origin of stem cells in the NP, CEP, and AF (including AFo), we chose this region as the target ISN area [24]. As expected, ISN-SCs exhibited characteristics that met the minimal criteria [27, 28] for multipotent mesenchymal stromal cells (MSCs). Such findings set the stage for intensive studies on self-regeneration in IVD.

Materials and methods

Isolation and culture of ISN-SCs and BMSCs

Sprague–Dawley (SD) rats (male, 10-week-old) were used for this study. All of the procedures specified below were

approved by the Institutional Animal Care and Use Committee of Southeast University (Nanjing, China). Animals were killed by an intraperitoneal overdose injection of 10 % chloral hydrate. For the isolation of ISN-SCs, the functional spinal units (FSUs) of L3–L6 were separated under aseptic conditions. The FSUs were then placed under a sterile dissecting microscope (Leica, Germany) to further remove the attached muscular and ligamentous tissues by ophthalmic surgical instruments. Moreover, IVD tissues, including the NP, AF, and CEP, were all carefully detached from the FSUs to expose the subchondral bone. After washing with phosphate-buffered saline (PBS) several times, tissues of the target ISN regions were separated with a surgical knife blade according to the anatomical areas previously described [24]. Specifically, the perichondrium region outside of the EP was separated from the secondary ossification center to 500 μm below that of the EP line (width, ∼100 μm; Figs. 1, 2). ISN tissues were then digested with 0.15 % collagenase II in Dulbecco's Modified Eagle Media: Nutrient Mixture F-12 (DMEM/F12, 1:1, Gibco, USA) containing 3 % fetal bovine serum (FBS, HyClone, USA) for 6 h at 37 °C. The suspension was then filtered using a 70-μm cell filter before centrifugation at 1000 rpm for 5 min. The cell pellet was then resuspended in DMEM/F12 supplemented with 10 % FBS and 1 % penicillin–streptomycin (Gibco, USA), and seeded into 25-cm^2 cell culture flasks maintained in a humidified incubator containing 5 % CO_2 at 37 °C. Medium was changed every 3 days, and the growth status of the cells was observed under an optical microscope. When cells reached 90 % confluency, they were harvested with 0.25 % trypsin/EDTA (Gibco, USA) and subcultured at 1:3. Passage 4 (P4) populations were used for subsequent analyses. For the isolation of BMSCs, femurs and tibias were
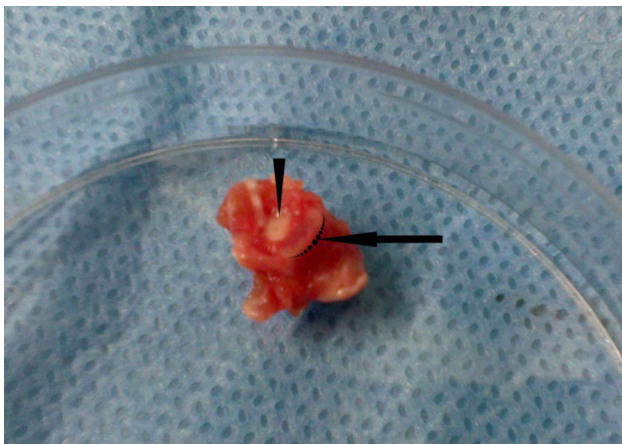

Fig. 2 The FSU was separated and the IVD tissues were carefully detached to expose the target ISN (the *black arc* area indicated by the *arrow*). The *white circular* region indicated by the *arrowhead* stands for spinal cord

harvested from the animals, a 22-gauge needle was inserted into the medullary space, bone marrow was then flushed out with 1 mL PBS. After being size-fractionated using Ficoll-Paque PLUS (1.077 g/mL, GE Healthcare Life Sciences), BMSCs were isolated by centrifugation for 30 min at room temperature. Cells were cultured in DMEM/F12 supplemented with 10 % FBS and 1 % penicillin–streptomycin (Gibco, USA), incubated in a humidified incubator containing 5 % CO_2 at 37 °C. P4 populations were used for further analyses.

Colony-forming assay

To compare the colony-forming abilities of ISN-SCs and BMSCs, P4 populations were plated in cell culture dishes at various seeding densities (100, 500, 1000, and 2000 cells/10 cm^2). After growth in culture for 14 days, crystal violet staining was performed to count the cell colonies as previously described [29]. Briefly, cells were washed three times with PBS, fixed in 4 % paraformaldehyde for 15 min, stained with 0.1 % crystal violet (Keygen Biotech, Nanjing, China) for 15 min, and washed twice with PBS before counting the number of colonies. A colony containing less than 30 cells was ignored. Colony-forming efficiency was calculated by dividing the number of colonies by the initial number of adherent cells.

Proliferation assay

To compare the proliferation abilities of ISN-SCs and BMSCs, the 3-(4, 5-dimethylthiazol-2-yl)-2, 5-diphenyltetrazolium bromide (MTT) method was used [30]. P4 cells were plated in 96-well cell culture plates at a density of 1000 cells/well, and were cultured in a humidified incubator. Wells were divided into 10 groups assigned to different time points (days 1–10). At each time point, 20 μL MTT (5 mg/mL, Sigma, USA) was added to each well of the corresponding group before incubation at 37 °C for 4 h. The medium containing MTT was aspirated, and 150 μL dimethyl sulfoxide (DMSO, Sigma) was added to the wells prior to incubation at 37 °C for 30 min. Finally, cell proliferation was determined by measuring the optical density (OD) values at 492 nm using a microplate reader (Thermo Scientific, USA).

Cell cycle assay

Cell cycle analysis was performed using the Cell Cycle Detection Kit (Keygen Biotech, Nanjing, China) according to the manufacturer's instructions. Briefly, at least 2×10^5 P4 cells were harvested and washed with PBS before resuspension in 100 μL PBS. The cell suspension (50 μL) was then transferred into a 15-mL sterile centrifuge tube.

Reagents A, B, and C were added sequentially, and incubated at room temperature (RT). Measurements were carried out on a FACSCalibur flow cytometer (BD, USA). Data were acquired by CellQuest software (BD, USA), and cell cycle distribution was analyzed by ModFit software (Verity Software House, USA).

Identification of immunophenotypes

To compare the immunophenotypes of ISN-SCs and BMSCs, P4 cells were harvested and washed with PBS. Every 1×10^6 cells were transferred into a 15-mL centrifuge tube and resuspended in 100 μL cold PBS. Phycoerythrin (PE)- and fluorescein isothiocyanate (FITC)-coupled monoclonal antibodies were added to the corresponding tubes, and were incubated with the cell suspension at 4 °C for 30 min in the dark. Isotype control antibodies served as controls. Cells were washed with cold PBS, and were resuspended in 300 μL cold PBS for single-channel flow cytometry (FCM) analysis (BD, USA). The percentage of positively stained cells was calculated relative to the isotype control. Fluorochrome-coupled anti-rat monoclonal antibodies, including CD29-PE, CD90-PE, and CD45-PE were purchased from eBioscience (USA). CD34-PE, CD44-PE, and CD19-FITC were purchased from Abcam (USA), and CD11b-FITC was purchased from BD Biosciences (Shanghai, China).

Identification of multipotential differentiation capacities

Osteogenic differentiation

Induction procedure Passage 4 cells were harvested with 0.25 % trypsin/EDTA, seeded into multi-well cell culture plates, and cultured in growth medium (DMEM/F12 supplemented with 10 % FBS and 1 % penicillin–streptomycin) at 37 °C in a 5 % CO_2 humidified incubator. After 24 h, when the cells were adherent, the growth medium was carefully aspirated from each well, and SD Rat Mesenchymal Stem Cell Osteogenic Differentiation Medium (10 % FBS, 1 % penicillin–streptomycin, 0.01 % dexamethasone, 1 % β-glycerophosphate, and 0.2 % ascorbate; Cyagen Biosciences, Guangzhou, China) was added. Cells were re-fed every 3 days with fresh differentiation medium over the total induction period of osteogenic differentiation (3 weeks). Cells cultured with growth medium only served as controls.

Quantitative analysis of alizarin red staining for mineralization To quantitatively determine the degree of mineralization, P4 cells were seeded into 96-well plates at a density of 1.5×10^4 cells/well, and subsequently underwent the osteogenic induction procedure described above. At the end of the induction period, the Stem Cell Osteogenic Differentiation Quantitative Detection Kit (Genmed, Shanghai, China) was used for further analysis according to the manufacturer's instructions. The wells were washed carefully with cleaning fluid prior to fixation (fluid was pre-chilled at −20 °C). After incubation for 60 min at −20 °C, the fixation fluid was aspirated, and wells were cleaned gently followed by the addition of alizarin red for 10 min at RT. The dye solution was then aspirated and wells were cleaned thoroughly. Alizarin red staining was observed under a microscope. Finally, lysis fluid was added to the wells, and cells were incubated on a shaking table at 50 revolutions per minute (RPM) for 15 min at RT. The intensity of the dissolved dye was immediately determined by measuring OD values at 562 nm in a microplate reader.

Calcium cobalt staining for alkaline phosphatase A Calcium Cobalt Staining Kit (Keygen Biotech, Nanjing, China) was used for the qualitative detection of alkaline phosphatase (ALP). P4 cells were harvested and seeded into 24-well plates at a density of 6×10^4 cells/well. When the 3-week osteogenic induction period was complete, the staining procedure was performed according to the manufacturer's instructions. Briefly, cells were fixed in 70 % alcohol, washed with distilled water, and incubated in incubation working liquid at 37 °C for 180 min. After washing with distilled water for 5–10 min, staining solution A (cobalt nitrate) was added for 5 min at RT. Wells were subsequently washed, and staining solution B (ammonium sulfide) was added. After incubation at RT for 1 min and washing for 5 min, the staining results were observed under a microscope.

Chondrogenic differentiation

Induction procedure Passage 4 cells were harvested, seeded into multi-well cell culture plates, and cultured in growth medium at 37 °C in a 5 % CO_2 humidified incubator. After 24 h, the growth medium was replaced with SD rat mesenchymal stem cell chondrogenic differentiation medium (0.01 % dexamethasone, 0.3 % ascorbate, 1 % ITS + Supplement, 0.1 % sodium pyruvate, 0.1 % proline, and 1 % TGF-β3; Cyagen Biosciences, Guangzhou, China). Cells were re-fed every 3 days with fresh differentiation medium over the total induction period of chondrogenic differentiation (3 weeks). Cells cultured with growth medium only served as controls.

Quantitative analysis of alcian blue staining for aggrecan To quantitatively determine chondrogenesis capacity, the extent of alcian blue staining for aggrecan was

determined using the Stem Cell Chondrogenic Differentiation Quantitative Detection Kit (Genmed, Shanghai, China) according to the manufacturer's instructions. P4 cells were seeded into 96-well plates at a density of 2×10^4 cells/well, and underwent the chondrogenic induction procedure described above. When the 3-week induction period was complete, cells were cleaned, fixed, and incubated at $-20\ °C$ for 60 min as described above. After aspirating the fixing solution, the dye solution (alcian blue) was added for 15 min at RT. The dye solution was then aspirated, and wells were thoroughly cleaned. Alcian blue staining was then observed under a microscope. Finally, the dye was dissolved by incubating with lysis fluid on a shaking table at 50 RPM for 30 min at RT. OD (595 nm) was immediately measured in a microplate reader.

Adipogenic differentiation

Induction procedure Passage 4 cells were harvested and seeded into multi-well plates, and cultured in growth medium at $37\ °C$ in a 5 % CO_2 humidified incubator. Cells were re-fed every 3 days until reaching 100 % confluency. The induction procedure began 4 days post-confluency with SD rat mesenchymal stem cell adipogenic differentiation medium A (induction medium; Cyagen Biosciences, Guangzhou, China) containing 10 % FBS, 1 % penicillin–streptomycin, 1 % glutamine, 0.2 % insulin, 0.1 % IBMX, 0.1 % rosiglitazone, and 0.1 % dexamethasone. After incubation in the induction medium for 72 h, medium was replaced with adipogenic differentiation medium B (maintenance medium; 10 % FBS, 1 % penicillin–streptomycin, 1 % glutamine, and 0.2 % insulin; Cyagen Biosciences, Guangzhou, China) for 24 h. This 96-h induction-maintenance cycle was repeated four times before the cells were incubated in maintenance medium for 7 days. Cells cultured with growth medium only served as controls.

Quantitative analysis of oil red O staining for lipid droplets The Stem Cell Adipogenic Differentiation Quantitative Detection Kit (Genmed, Shanghai, China) was used to quantitatively determine adipogenic differentiation ability by detecting the extent of oil red O staining. P4 cells were seeded into 96-well plates at a density of 1.5×10^4 cells/well, and underwent the induction procedure described above. Briefly, the wells were cleaned, fixed, and stained with oil red O for 15 min at RT before being observed under a microscope and lysed on a shaking table at 50 RPM at RT for 30 min. OD values at 520 nm were then measured in a BioRad reader.

Quantitative real-time polymerase chain reaction Quantitative real-time polymerase chain reaction (qPCR) was used to determine relative gene expression. The expression of stem cell-related genes (NANOG, SOX-2, and OCT-4) was compared between P4 BMSCs and ISN-SCs. In addition, the expression of multipotential differentiation-related genes, including those related to osteogenesis (Runx2, OPN and OCN), chondrogenesis (SOX-9, COL2a1, and ACAN), and adipogenesis (PPARγ and C/EBPα) were compared between induced and control groups. Cells were harvested, and total RNA was extracted using TRIzol reagent (Invitrogen, USA). RNA (5 μL) was then added to 595 μL 1 × TE buffer before measuring OD values at 260 nm and 280 nm on a spectrophotometer (Shimadzu UV-2450, Kyoto, Japan). RNA (2 μg) was used for cDNA synthesis using a Gradient PCR instrument (ABI Veriti 96-well Thermal cycler, USA). Real-time PCR was then performed in a final volume of 20 μL including 10 μL 2X Real-time PCR Master Mix (SYBR Green, TOYOBO, Osaka, Japan), 1 μL cDNA (diluted 10:1), 2 μL primer mix (F/R, 1:1; concentration, 10 μM), and 7 μL 0.1 % DEPC-treated water. Each reaction was performed in triplicate. The housekeeping gene GAPDH was used for normalization. The $2^{-\Delta\Delta CT}$ method was used to calculate the expression level of each target gene. Primer sequences of the target genes were designed by Primer Premier 5.0 (Premier, Canada) and synthesized by GenScript Biotechnology (Nanjing, China). Detailed information on the primers is shown in Table 1.

Statistical analysis

Each experiment was replicated at least three times. Quantitative data are presented as the mean ± standard deviation (SD). Statistical analyses were performed using SPSS version 20.0. Student's t test was used to compare the quantifiable data between groups. p values less than 0.05 were considered statistically significant.

Results

Morphologies and colony-forming abilities of rat ISN-SCs and BMSCs

After growing in culture for 4 days, both primary ISN-SCs and BMSCs gradually formed colonies. Primary cells were subcultured for approximately 10 days following the initial seeding when the colonies were too intensive to extend. The interval between adjacent passages was approximately 7 days thereafter. P4 ISN-SCs appeared as fibroblast-like cells with multi-tentacles forming vortexes partially under general observation, and P4 BMSCs appeared as the similar morphology but with more slender shapes (Fig. 3). The colony-forming assay showed that both of ISN-SCs and

Table 1 Sequences of primers for qPCR

Target gene	Size (bp)	Primers sequences	T_A (°C)	Cycles
GAPDH	103	Sense: 5′-GGCCTTCCGTGTTCCTACC-3′	60	40
		Antisense: 5′-CGCCTGCTTCACCACCTTC-3′		
NANOG	76	Sense: 5′-TGGTTGAAGACTAGCAACGG-3′	60	40
		Antisense: 5′-AATAGCTGCAATGGATGCTG-3′		
SOX-2	117	Sense: 5′-AGCAAGTACTGGCAAGACCA-3′	60	40
		Antisense: 5′-CGATATCAACCTGCATGGAC-3′		
OCT-4	104	Sense: 5′-GAGGAAGCTGACAACAACGA-3′	60	40
		Antisense: 5′-CACCTCACACGGTTCTCAAT-3′		
Runx2	138	Sense: 5′-GCGTCCTATCAGTTCCCAAT-3′	60	40
		Antisense: 5′-ATCAGCGTCAACACCATCAT-3′		
OPN	103	Sense: 5′-TCCAGGAGTTTCCCTGTTTC-3′	60	40
		Antisense: 5′-TGACCTTGATAGCCTCATCG-3′		
OCN	70	Sense: 5′-CCTAGCAGACACCATGAGGA-3′	60	40
		Antisense: 5′-GTCAGAGAGGCAGAATGCAG-3′		
ACAN	74	Sense: 5′-GGAGAAGAGACCCAAACAGC-3′	60	40
		Antisense: 5′-GACCCTTCTGGAGAAGCAAG-3′		
COL2a1	70	Sense: 5′-GGAAGAGCGGAGACTACTGG-3′	60	40
		Antisense: 5′-TTGCAGAAGACTTTCATGGC-3′		
SOX-9	110	Sense: 5′-GCCTGGACTGTATGTGGATG-3′	60	40
		Antisense: 5′-TCTGTCCGATGTCTCTCTGC-3′		
PPARγ	99	Sense: 5′-TCTCACAATGCCATCAGGTT-3′	60	40
		Antisense: 5′-AGACTCTGGGTTCAGCTGGT-3′		
C/EBPα	101	Sense: 5′-CCAGAAGGCTGAGTTGTGAA-3′	60	40
		Antisense: 5′-GGTCCCAGTGTCTTCATCCT-3′		
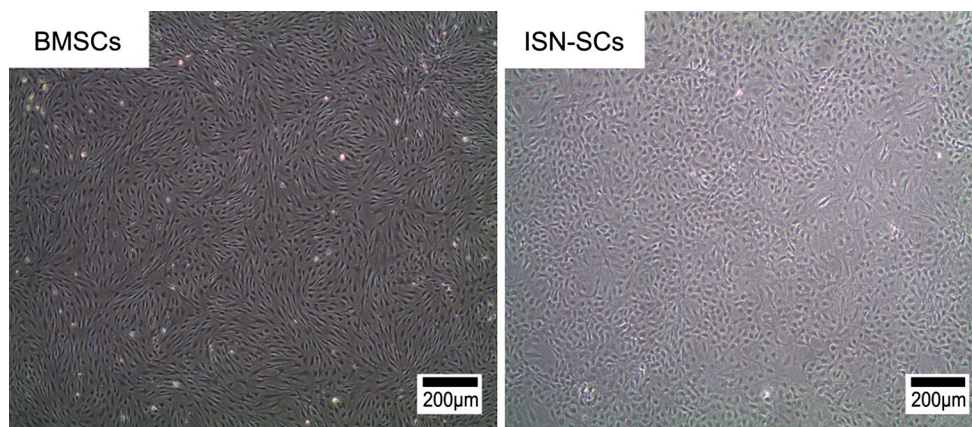
Fig. 3 Morphologies of P4 ISN-SCs and BMSCs. The ISN-SCs were fibroblast-like cells with multi-tentacles forming vortexes partially, and BMSCs appeared as the similar morphology but with more slender shapes

BMSCs acquired optimal colony-forming efficiencies (23.3 and 25.7 %, respectively; $p > 0.05$) at the initial seeding densities of 100 cells/10 cm^2. The efficiencies gradually declined as the initial seeding density increased, and BMSCs showed significantly better colony-forming abilities at the initial seeding densities of 500, 1000 and 2000 cells/10 cm^2 (Fig. 4).

Cell cycle analysis and proliferation of rat ISN-SCs and BMSCs

Flow cytometry analysis (Fig. 5) revealed that both of ISN-SCs and BMSCs were mainly in the G0/G1 phase (>80 %). The percentage of cells in G0/G1 phase was even significantly higher in ISN-SCs than that in BMSCs

Fig. 4 Colony forming of ISN-SCs and BMSCs. **a** Colonies stained with crystal *violet* at 14 days after initial seeding of the cells at different densities. **b** Colony-forming efficiencies of ISN-SCs and BMSCs at different initial seeding densities. *$p < 0.05$ was considered as a significant difference between compared groups
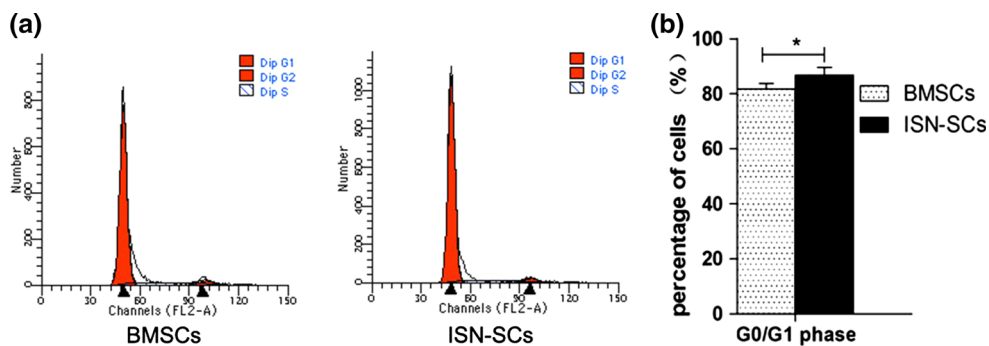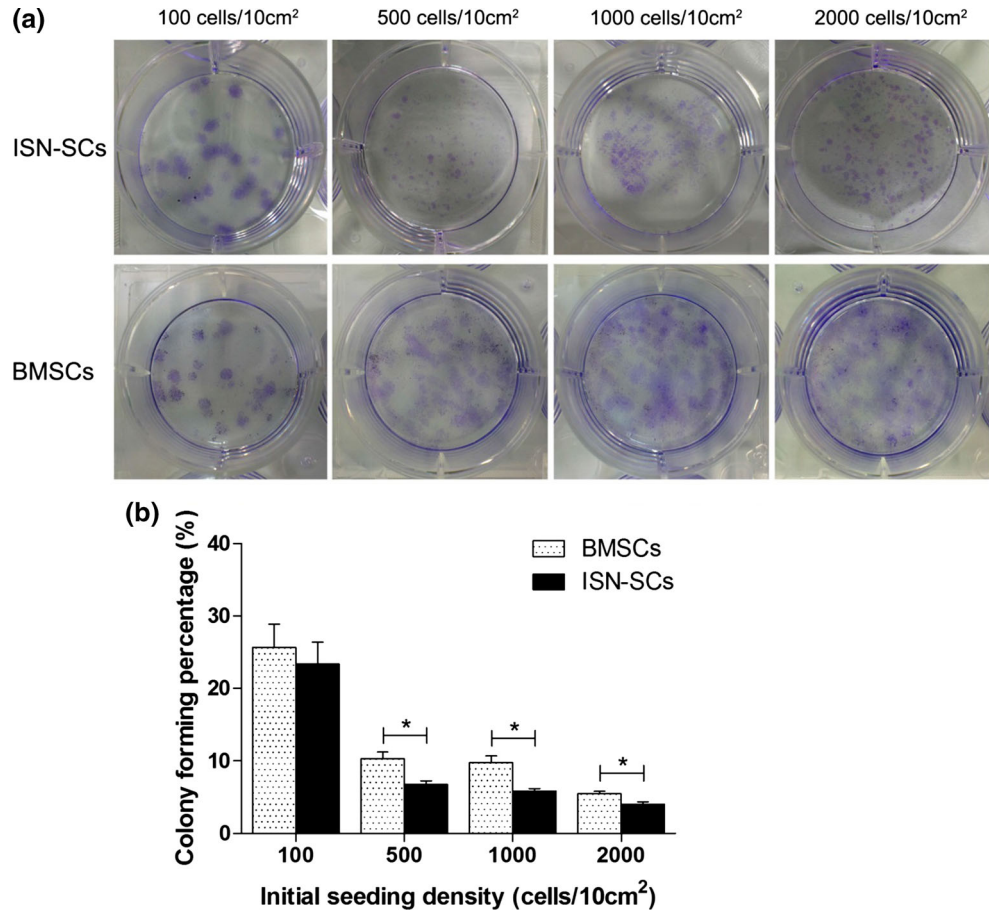

Fig. 5 Cell cycles of ISN-SCs and BMSCs determined by FCM analysis. **a** Representative graphs of cell cycles. **b** Comparison of G0/G1 phases between ISN-SCs and BMSCs, a significantly larger proportion of cells in G0/G1 phase was observed in ISN-SCs, but both of them were mainly in the G0/G1 phase (>80 %). *$p < 0.05$ was considered as a significant difference between compared groups

(86.75 ± 2.81 versus 81.60 ± 2.07 %; $p < 0.05$), whereas only a small percentage of the cell population was undergoing proliferation (S, G2, and M). Regarding the proliferation abilities of ISN-SCs and BMSCs, the MTT assay (Fig. 6) showed that both of ISN-SCs and BMSCs experienced a slow growing period during the initial 3 days before converting into a log phase. Ultimately, the growing speed slowed again, representing an S-shape growth curve.

Moreover, the OD values of BMSCs were significantly stronger than that of ISN-SCs from day 3 to day 10, representing a better proliferation ability of BMSCs.

Features of immunophenotypes

The expression of cell surface antigens was also analyzed by FCM (Figs. 7, 8). Both of ISN-SCs and BMSCs were
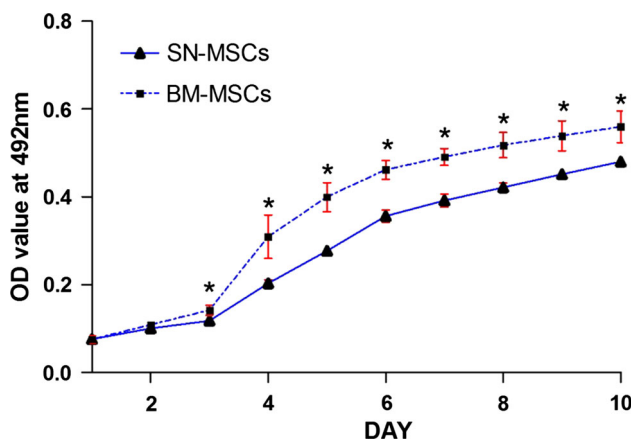
Fig. 6 Growth curves of P4 ISN-SCs and BMSCs determined by the MTT method. The OD values of BMSCs were significantly stronger than that of ISN-SCs from day 3 to day 10, representing a better proliferation ability of BMSCs. *$p < 0.05$ was considered as a significant difference between compared groups

highly positive ($\geq$95 %) for stem cell markers CD29 and CD90, and slightly positive ($\leq$2 %) for the negative markers CD34, CD45, CD19, and CD11b. Particularly, BMSCs expressed significantly higher CD44 than ISN-SCs (99.17 ± 0.81 versus 87.57 ± 1.96 %; $p < 0.05$).

Multipotential differentiation capacities

Osteogenic differentiation

At the end of the osteogenic induction procedure, crowds of calcium nodules were observed in both of induced ISN-SCs and BMSCs by alizarin red staining (Fig. 9a). Further quantitative analysis (Fig. 10a) showed that both of the induced ISN-SCs and BMSCs groups exhibited much stronger OD values at 562 nm compared to the controls ($p < 0.05$). Moreover, the OD value of induced ISN-SCs was significantly stronger than that of induced BMSCs. In addition, the calcium cobalt staining method for ALP revealed that extensively stained areas, which were absent in the control groups, emerged in both of induced ISN-SCs and BMSCs (Fig. 9b).

Chondrogenic differentiation

After the chondrogenic induction period, alcian blue staining for aggrecan was used to determine chondrogenic differentiation abilities. Both of the induced ISN-SCs and BMSCs were intensively stained, whereas only a few cells were observed in the controls (Fig. 9c); this was in accordance with the quantitative analysis (Fig. 10b) presenting stronger OD values at 595 nm in both of the induced ISN-SCs and BMSCs groups compared to the

controls ($p < 0.05$). Moreover, the OD value of induced ISN-SCs was significantly stronger than that of induced BMSCs.

Adipogenic differentiation

At the end of the adipogenic induction period, oil red O staining showed that a range of lipid droplets developed in both of the induced ISN-SCs and BMSCs groups, but not in the control group (Fig. 9d). Similarly, quantitative analysis (Fig. 10c) revealed stronger OD values at 520 nm in both of the induced ISN-SCs and BMSCs groups compared to the controls ($p < 0.05$). No significant difference of the OD values was observed between induced ISN-SCs and BMSCs.

qPCR analysis

Quantitative real-time polymerase chain reaction analysis showed that the ISN-SCs expressed comparable stem cell-related genes relative to BMSCs with respect to SOX-2 and OCT-4. Furthermore, increased expression of NANOG was observed in ISN-SCs ($p < 0.05$, Fig. 11a). Regarding the expression of multipotential differentiation-related genes (Fig. 11b–i) in ISN-SCs and BMSCs, the results showed that Runx2, OPN, and OCN (osteogenic induction group), SOX-9, COL2a1, and ACAN (chondrogenic induction group), and PPARγ and C/EBPα (adipogenic induction group) were significantly increased in both induced ISN-SCs and BMSCs relative to the controls ($p < 0.05$). When compared to induced BMSCs, induced ISN-SCs expressed higher levels of osteogenesis- and chondrogenesis-related genes ($p < 0.05$), but no difference was observed regarding to adipogenesis-related genes. These findings were in accordance with the quantitative analysis results of multipotential differentiation capacities, representing stronger osteogenic and chondrogenic differentiation capacities of ISN-SCs compared to those of BMSCs. Besides, when compared to control group of BMSCs, control group of ISN-SCs expressed higher levels of OCN, SOX-9, COL2a1, and ACAN ($p < 0.05$).

Discussion

With increasing knowledge on stem cell transplantation, cell-based therapeutic approaches are becoming promising strategies for IVDD regeneration [5, 6]. Another stem cell-based approach, which has been applied to the regeneration of many other tissues, aims to promote endogenous stem cell migration to the target area. However, few studies examined endogenous stem cell migration into the IVD until the potential ISN was proposed [21]. Nevertheless,
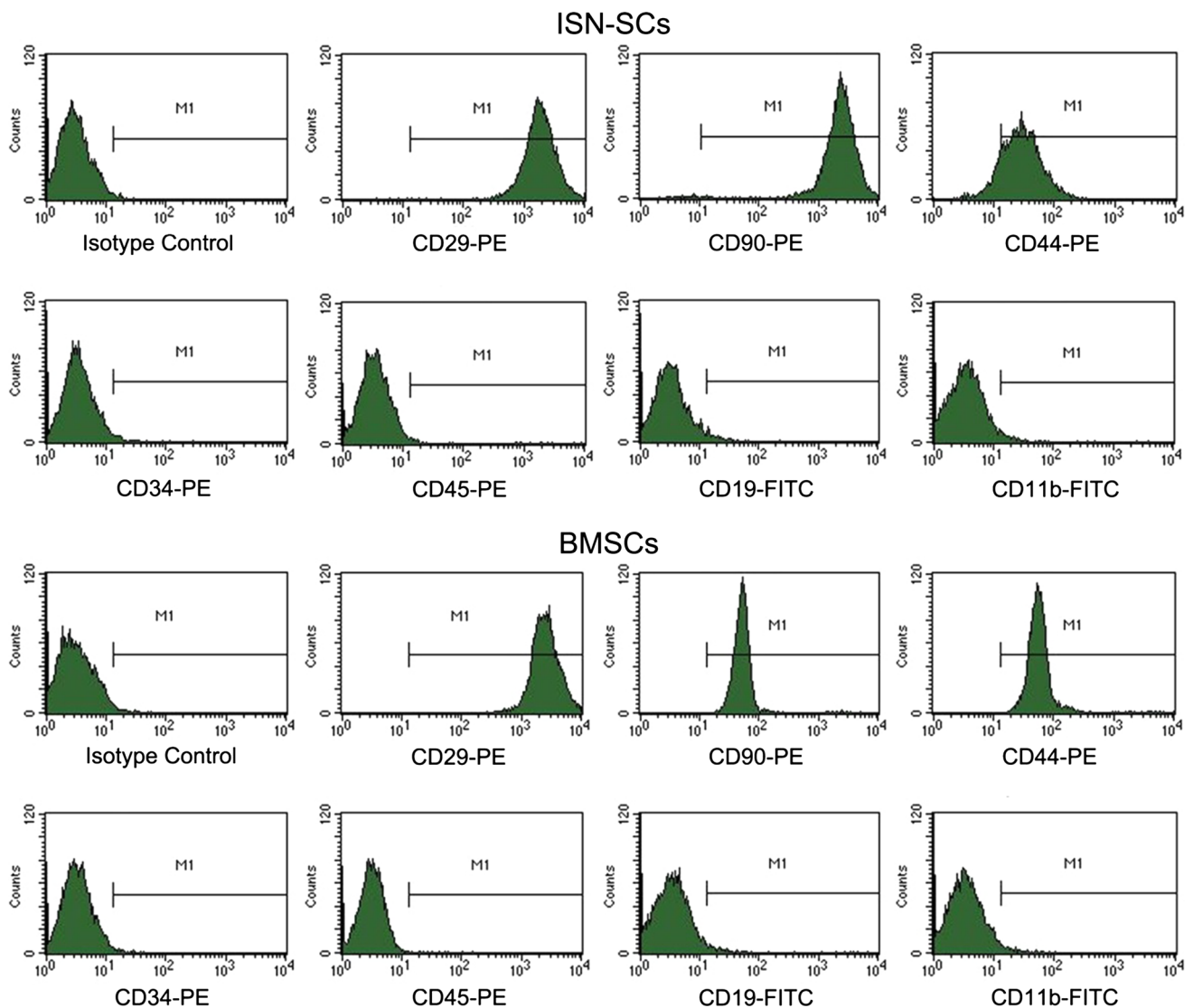
Fig. 7 Immunophenotypes of ISN-SCs and BMSCs determined by FCM analysis. The percentage of positively stained cells was calculated relative to the isotype control

ISN-SC characteristics are unknown due to a lack of in vitro studies. In this in vitro study, ISN-SCs from rats were successfully isolated and compared with BMSCs with respect to colony-forming ability, cellular immunophenotypes, cell cycle, stem cell-related gene expression, and proliferation and multipotential differentiation capacities.

Primary ISN-SCs mainly existed in the shape of crowds of colonies adherent to the wall of the plastic cell culture flask approximately 4 days after the initial seeding, which is in accordance with the first minimal criteria for defining MSCs proposed by the International Society for Cellular Therapy (ISCT) [27]. With respect to cellular morphology, ISN-SCs mainly appeared as fibroblast-like cells with multi-tentacles forming a vortex partially under general

observation, displaying excellent homogeneity. And BMSCs appeared as the similar morphology but with more slender shapes. In addition, the fibroblast-like cell morphology is consistent with cells originating from the AFo area, as described in an earlier study [31]. It should be noted that the AFo represents another potential ISN region that we did not choose as the target site in this study. Therefore, the potential ISN, including the AFo and perichondrium region adjacent to the EP (target ISN in this study), may possess stem cells with the same morphology. Regarding colony-forming ability, both of ISN-SCs and BMSCs acquired optimal colony-forming efficiencies (23.3 and 25.7 %, respectively) without statistical significance at the initial seeding densities of 100 cells/10 cm² , indicating
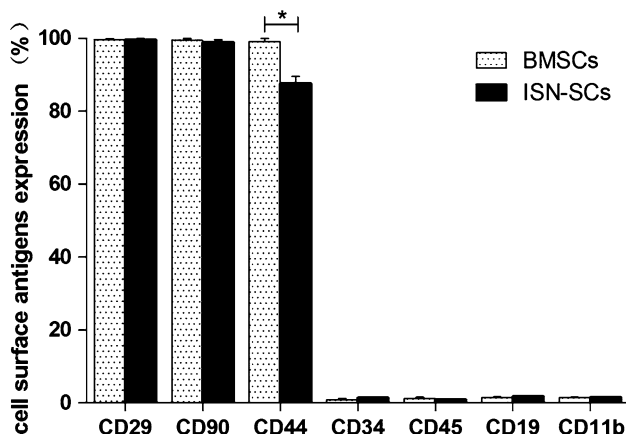
Fig. 8 The mean values of cell surface antigens expression. *$p < 0.05$ was considered as a significant difference between compared groups

a more powerful colony-forming capacity relative to the stem cells derived from other tissues as described in previous studies [29, 32].

The specific immunophenotypic features represent the second criteria for defining MSCs proposed by the ISCT [27]. In the present study, FCM showed that both of ISN-SCs and BMSCs fulfilled the majority of requirements regarding the expression of specific surface antigen molecules. The population of both cell types were positive for CD90 (>98 %), and were negative (≤2 %) for CD34, CD45, CD19, and CD11b, consistent with the criteria described above. The other two positive stem cell markers, CD73 and CD105, were not detected due to the difficulty of acquiring fluorochrome-coupled anti-rat antibodies. Thus, two additional positive markers (CD29 and CD44) were chosen for analysis due to their stable, positive expression in MSCs from rats, as described in a recent review [28]. CD29 expression of ISN-SCs was comparable to that of BMSCs and stem cells from different tissues examined in other studies [33–35]. CD44 was mainly positive in ISN-SCs (87.57 ± 1.96 %), which was significantly lower than that in BMSCs (99.17 ± 0.81 %) and with minor differences compared to previous findings [18, 35]. Minor differences in CD44 expression were also observed in previous studies on stem cells from different species, tissues, and even the same cells from different passages [18, 35, 36]. These differences may be caused by the varying culture conditions and possibly even cellular functions [18]. Considering that CD44 is correlated with stem cell migration [37], and that BMSCs (with high expression of CD44) have exhibited excellent functional performance of migration [38, 39], the high expression of CD44 may also indicate a superior migration function of ISN-SCs, which is crucial in the process of self-regeneration in the IVD.

The third requirement for defining MSCs suggested by the ISCT is the multilineage differentiation capacity [27].

Our present study demonstrated that both of ISN-SCs and BMSCs possess the multipotential differentiation abilities with respect to osteogenesis, chondrogenesis, and adipogenesis. The osteogenic efficiency was determined by alizarin red staining for mineralization and calcium cobalt staining for ALP, and the effects of chondrogenesis and adipogenesis were detected by alcian blue staining for aggrecan and oil red O staining for lipid droplets, respectively, which are commonly used for the detection of multilineage potential [18, 40]. It should be noted that, in the chondrogenic test, parts of the ISN-SCs and BMSCs from the control groups cultured in the growth medium were also stained blue, indicating an intrinsic characteristic of self-transformation into chondrocyte-like cells. And further qPCR analysis revealed that the levels of chondrogenesis-related genes (SOX-9, COL2a1 and ACAN) expression were significantly higher in the control group of ISN-SCs than those in the control group of BMSCs, representing a stronger self-chondrogenic capacity of ISN-SCs. This may be of great meaning in the process of self-regeneration in the IVD, which mainly consists of a chondrocyte-like cell population. Furthermore, quantitative analysis for comparing the extent of staining between induced and control groups demonstrated strong multilineage differentiation efficiencies of ISN-SCs and BMSCs. These were further confirmed by qPCR analysis, which revealed significantly increased expression of multipotential differentiation-related genes in the induced groups, including osteogenesis (Runx2, OPN, and OCN)-, chondrogenesis (SOX-9, COL2a1 and ACAN)- and adipogenesis (PPARγ and C/EBPα)-related genes that were universally used in previous studies on the multilineage differentiation of stem cells [18, 20]. Particularly, both of quantitative analysis for comparing the extent of staining and qPCR analysis demonstrated more powerful osteogenic and chondrogenic abilities of ISN-SCs than those of BMSCs. Thus, ISN-SCs may provide promising results in the process of self-regeneration in the IVD.

In addition to the three minimal criteria for defining MSCs presented by the ISCT, we also examined colony-forming and proliferation capacities, as well as cell cycle and stem cell-related gene expression, which may be of concern in determining the characteristics and 'stemness' of ISN-SCs. Stem cells are slow cycling cells, featured by the majority of cells staying in the resting stage (G0/G1 phase), which is closely related to cell pluripotency [41]. A previous study demonstrated that both BMSCs and stem cells derived from the CEP were mainly in the G0/G1 phase [18]. In this study, FCM analysis showed similar results, in which the majority of ISN-SCs and BMSCs were in the G0/G1 phase (>80 %), the percentage of cells in G0/G1 phase was even significantly higher in ISN-SCs than that in BMSCs, and only a
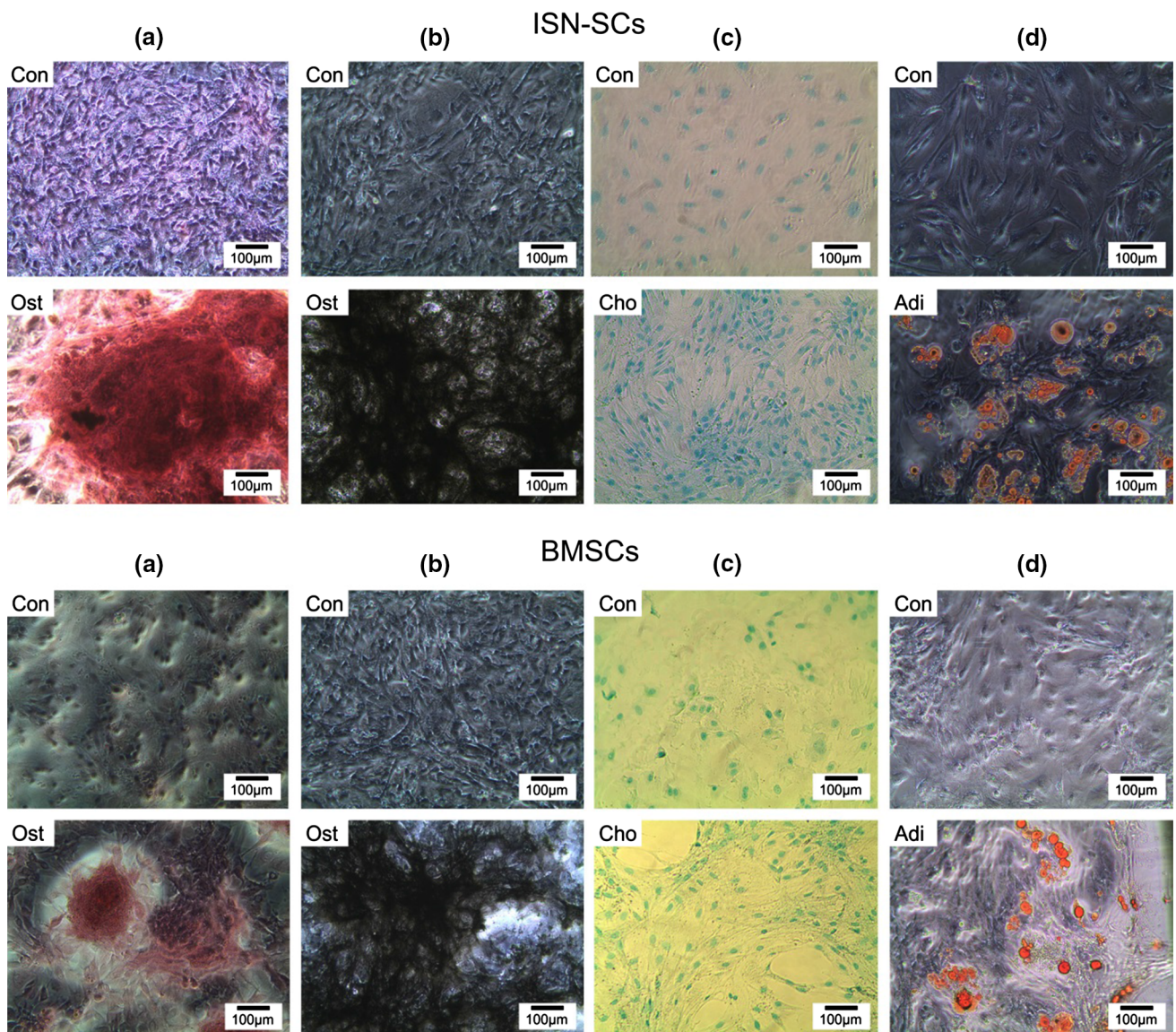
Fig. 9 Induced multilineage differentiation capacities of ISN-SCs and BMSCs. **a** Alizarin red staining for calcium nodus. **b** Calcium cobalt staining for ALP. **c** Alcian blue staining for aggrecan. **d** Oil red O staining for lipid droplets. *Con* control group, *Ost* osteogenic induction group, *Cho* chondrogenic induction group, *Adi* adipogenic induction group
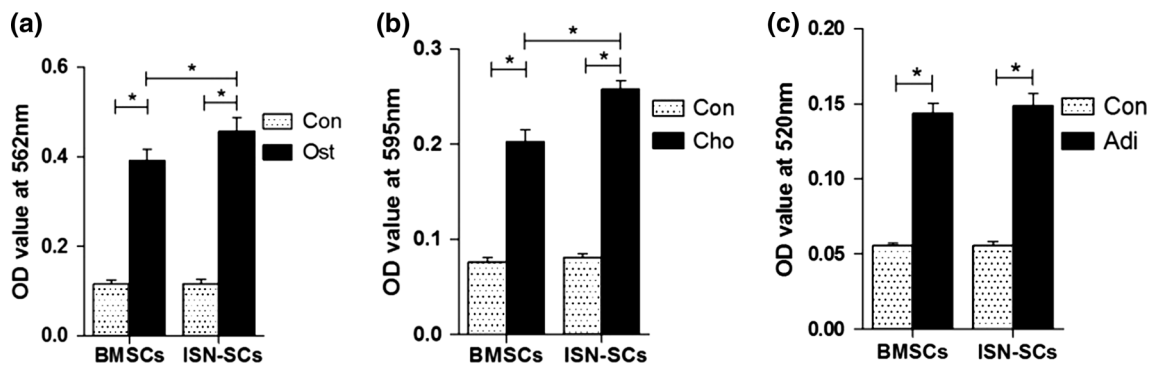

Fig. 10 Quantitative analysis of multilineage differentiation capacities of ISN-SCs and BMSCs with respect to osteogenesis (**a**), chondrogenesis (**b**) and adipogenesis (**c**). *Con* control group, *Ost* osteogenic induction group, *Cho* chondrogenic induction group, *Adi* adipogenic induction group. *$p < 0.05$ was considered as a significant difference between compared groups
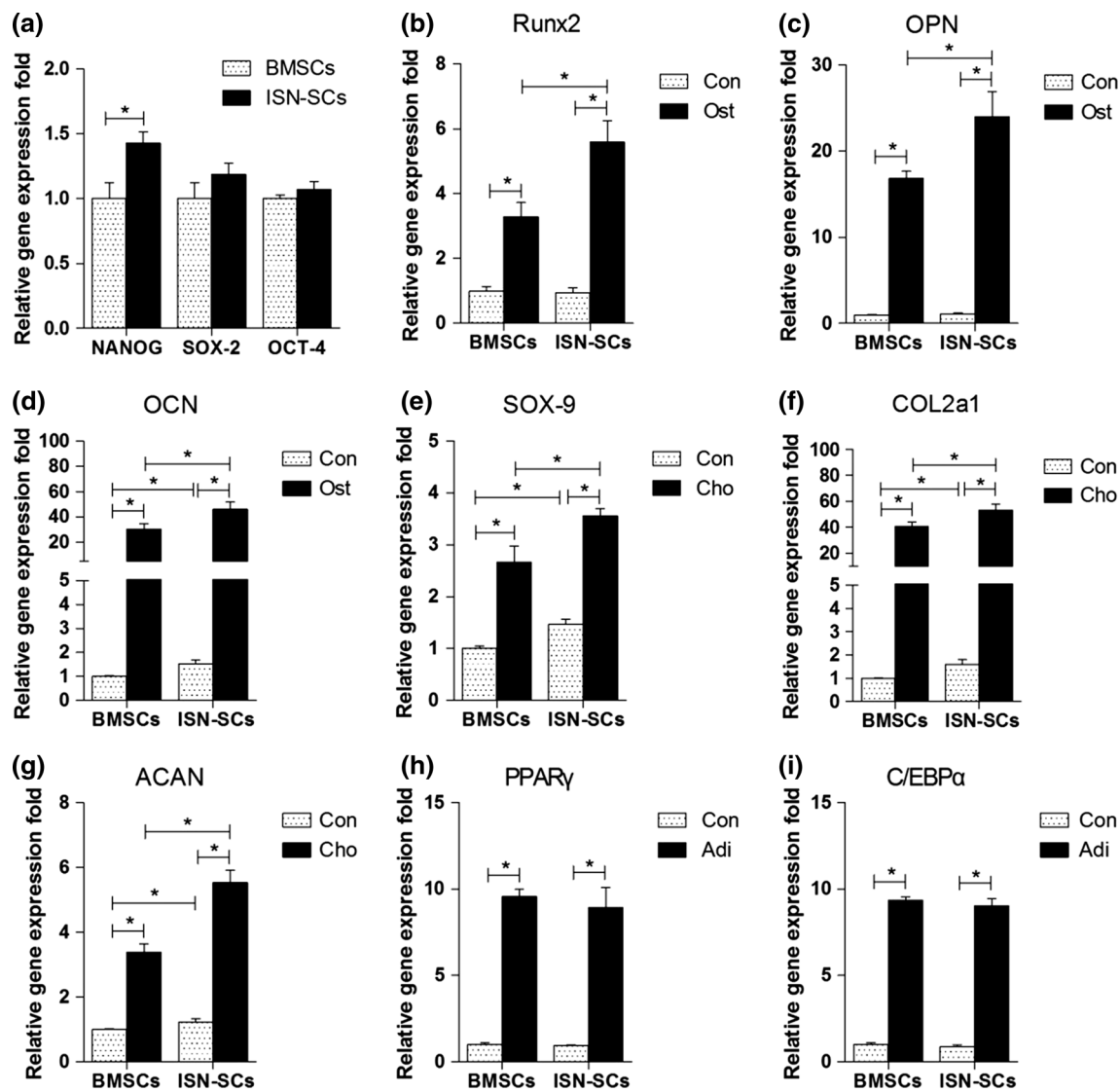
Fig. 11 The mRNA levels of the target genes analyzed by qPCR. **a** Comparison of stem cell-related gene expression between BMSCs and ISN-SCs. ISN-SCs expressed comparable stem cell-related genes relative to BMSCs with respect to SOX-2 and OCT-4. Furthermore, a significantly increased expression of NANOG was observed in ISN-SCs. **b–d** Comparison of osteogenesis-related genes (Runx2, OPN, and OCN) expression between compared groups. **e–g** Comparison of chondrogenesis-related genes (SOX-9, COL2a1, and ACAN) expression between compared groups. **h–i** Comparison of adipogenesis-related genes (PPARγ and C/EBPα) expression between compared groups. *Con* control group, *Ost* osteogenic induction group, *Cho* chondrogenic induction group, *Adi* adipogenic induction group. $*p < 0.05$ was considered as a significant difference between compared groups

small portion of the cell population was in a proliferative state (S, G2, and M phases). This result is in accordance with previous in vivo studies of labeling slow cycling cells in the ISN region [21, 23, 24], further demonstrating the existence of stem cells in the potential ISN. Cell proliferation, as determined by the MTT assay, presented an S-shaped growth curve of both ISN-SCs and BMSCs with a logarithmic growth phase, similar to that of stem cells derived from other tissues as described in previous studies [20, 29], suggesting a strong proliferation ability of ISN-SCs, though a better results was observed in BMSCs. NANOG, SOX-2, and OCT-4 are transcription factors that cooperatively maintain the regulatory system of cell self-renewal and pluripotency [42]. In light of their high expression levels, they are also deemed as stem cell markers [43]. A recent study demonstrated stable, high expression of these three factors in BMSCs [44]. Therefore, the expression of NANOG, SOX-2, and OCT-4 in ISN-SCs were compared to those in BMSCs. ISN-SCs expressed comparable levels of SOX-2 and OCT-4 compared to BMSCs. Moreover, increased expression of NANOG, which is the gateway to the pluripotent status [45], was presented in ISN-SCs. These data further demonstrate the 'stem-ness' of ISN-SCs.

Despite the strength of our findings, some critical problems need to be emphasized. First, ISN tissues may be difficult to harvest from humans during operations due to their anatomic characteristics; this restricts the use of human ISN-SCs in tissue engineering for IVD repair. Therefore, future research should primarily focus on self-regeneration caused by internal migration of ISN-SCs into the IVD. Another problem relates to the aging of the SCN, which may result in a loss of stem cell self-renewal capacity in many types of tissues [46–48]; whether a similar aging process happens in the ISN and the underlying potential mechanism remain to be illustrated. Simultaneously, a new challenge will be the maintenance of the liveness of the ISN. Considering that supporting the self-regeneration of IVD is one of the potential functions of ISN-SCs, future studies should focus on its abilities of differentiation into NP and AF cells and repair effects on IVDD. Moreover, the migration ability, the impact of normal and degenerated IVD cells on the migration process, and the potential mechanisms are needed to be further determined. Besides, the different cellular content of IVDs across species cannot be neglected. For example, rats are known to retain notochordal cells almost throughout life (age at loss of notochordal cells is 12 months), while sheep and humans are not [49]. Although demonstrating promising initial results, whether results regarding ISN-SC may translate to an adult human disc still need to be investigated.

In summary, we successfully isolated and identified ISN-SCs for the first time. The results from this study demonstrate that ISN-SCs represent members of the MSC family, with greater osteogenic and chondrogenic abilities than BMSCs. This finding may be of great significance for future studies that investigate the migration of ISN-SCs into the IVD and the underlying mechanism, and may provide a new perspective on novel biological treatment strategies for IVDD.

Compliance with ethical standards

Conflict of interest None.

References

1. Luo X, Pietrobon R, Sun SX, Liu GG, Hey L (2004) Estimates and patterns of direct health care expenditures among individuals with back pain in the United States. Spine (Phila Pa 1976) 29(1):79–86. doi:10.1097/01.BRS.0000105527.13866.0F

2. Luoma K, Riihimaki H, Luukkonen R, Raininko R, Viikari-Juntura E, Lamminen A (2000) Low back pain in relation to lumbar disc degeneration. Spine (Phila Pa 1976) 25(4):487–492

3. Wang H, Zhou Y, Huang B, Liu LT, Liu MH, Wang J, Li CQ, Zhang ZF, Chu TW, Xiong CJ (2014) Utilization of stem cells in alginate for nucleus pulposus tissue engineering. Tissue Eng Part A 20(5–6):908–920. doi:10.1089/ten.TEA.2012.0703

4. Clarke LE, Richardson SM, Hoyland JA (2015) Harnessing the potential of mesenchymal stem cells for IVD regeneration. Curr Stem Cell Res Ther 10(4):296–306

5. Longo UG, Papapietro N, Petrillo S, Franceschetti E, Maffulli N, Denaro V (2012) Mesenchymal stem cell for prevention and management of intervertebral disc degeneration. Stem Cells Int 2012:921053. doi:10.1155/2012/921053

6. Cai F, Wu XT, Xie XH, Wang F, Hong X, Zhuang SY, Zhu L, Rui YF, Shi R (2015) Evaluation of intervertebral disc regeneration with implantation of bone marrow mesenchymal stem cells (BMSCs) using quantitative T2 mapping: a study in rabbits. Int Orthop 39(1):149–159. doi:10.1007/s00264-014-2481-0

7. Hoogendoorn RJW, Lu ZF, Kroeze RJ, Bank RA, Wuisman PI, Helder MN (2008) Adipose stem cells for intervertebral disc regeneration: current status and concepts for the future. J Cell Mol Med 12(6a):2205–2216. doi:10.1111/j.1582-4934.2008.00291.x

8. Song K, Gu T, Shuang F, Tang J, Ren D, Qin J, Hou S (2015) Adipose-derived stem cells improve the viability of nucleus pulposus cells in degenerated intervertebral discs. Mol Med Reports. doi:10.3892/mmr.2015.3895

9. Schofield R (1978) The relationship between the spleen colony-forming cell and the haematopoietic stem cell. Blood cells 4(1–2):7–25

10. Jedrzejas M, Skowron K, Czekaj P (2012) Stem cell niches exposed to tobacco smoke. Przegl Lek 69(10):1063–1073

11. Voog J, Jones DL (2010) Stem cells and the niche: a dynamic duo. Cell Stem Cell 6(2):103–115. doi:10.1016/j.stem.2010.01.011

12. Wang K, Zhao X, Kuang C, Qian D, Wang H, Jiang H, Deng M, Huang L (2012) Overexpression of SDF-1alpha enhanced migration and engraftment of cardiac stem cells and reduced infarcted size via CXCR4/PI3K pathway. PLoS ONE 7(9):e43922. doi:10.1371/journal.pone.0043922

13. Christie KJ, Turnley AM (2012) Regulation of endogenous neural stem/progenitor cells for neural repair—factors that promote neurogenesis and gliogenesis in the normal and damaged brain. Front Cell Neurosci 6:70. doi:10.3389/fncel.2012.00070

14. Madhavan L, Collier TJ (2010) A synergistic approach for neural repair: cell transplantation and induction of endogenous precursor cell activity. Neuropharmacology 58(6):835–844. doi:10.1016/j.neuropharm.2009.10.005

15. Saha B, Jaber M, Gaillard A (2012) Potentials of endogenous neural stem cells in cortical repair. Front Cell Neurosci 6:14. doi:10.3389/fncel.2012.00014

16. Yu H, Vu TH, Cho KS, Guo C, Chen DF (2014) Mobilizing endogenous stem cells for retinal repair. Transl Res 163(4):387–398. doi:10.1016/j.trsl.2013.11.011

17. Sakai D, Nakamura Y, Nakai T, Mishima T, Kato S, Grad S, Alini M, Risbud MV, Chan D, Cheah KS, Yamamura K, Masuda K, Okano H, Ando K, Mochida J (2012) Exhaustion of nucleus pulposus progenitor cells with ageing and degeneration of the intervertebral disc. Nat Commun 3:1264. doi:10.1038/ncomms2226

18. Liu LT, Huang B, Li CQ, Zhuang Y, Wang J, Zhou Y (2011) Characteristics of stem cells derived from the degenerated human intervertebral disc cartilage endplate. PLoS ONE 6(10):e26285. doi:10.1371/journal.pone.0026285

19. Huang B, Liu LT, Li CQ, Zhuang Y, Luo G, Hu SY, Zhou Y (2012) Study to determine the presence of progenitor cells in the degenerated human cartilage endplates. Eur Spine J 21(4):613–622. doi:10.1007/s00586-011-2039-4

20. Liu C, Guo Q, Li J, Wang S, Wang Y, Li B, Yang H (2014) Identification of rabbit annulus fibrosus-derived stem cells. PLoS ONE 9(9):e108239. doi:10.1371/journal.pone.0108239

21. Henriksson H, Thornemo M, Karlsson C, Hagg O, Junevik K, Lindahl A, Brisby H (2009) Identification of cell proliferation zones, progenitor cells and a potential stem cell niche in the intervertebral disc region: a study in four species. Spine (Phila Pa 1976) 34(21):2278–2287. doi:10.1097/BRS.0b013e3181a95ad2

22. Henriksson HB, Lindahl A, Skioldebrand E, Junevik K, Tangemo C, Mattsson J, Brisby H (2013) Similar cellular migration patterns from niches in intervertebral disc and in knee-joint regions detected by in situ labeling: an experimental study in the New Zealand white rabbit. Stem Cell Res Therapy 4(5):104. doi:10.1186/scrt315

23. Henriksson HB, Svala E, Skioldebrand E, Lindahl A, Brisby H (2012) Support of concept that migrating progenitor cells from stem cell niches contribute to normal regeneration of the adult mammal intervertebral disc: a descriptive study in the New Zealand white rabbit. Spine (Phila Pa 1976) 37(9):722–732. doi:10.1097/BRS.0b013e318231c2f7

24. Sasaki N, Henriksson HB, Runesson E, Larsson K, Sekiguchi M, Kikuchi S, Konno S, Rydevik B, Brisby H (2012) Physical exercise affects cell proliferation in lumbar intervertebral disc regions in rats. Spine (Phila Pa 1976) 37(17):1440–1447. doi:10.1097/BRS.0b013e31824ff87d

25. Ishii Y, Thomas AO, Guo XE, Hung CT, Chen FH (2006) Localization and distribution of cartilage oligomeric matrix protein in the rat intervertebral disc. Spine (Phila Pa 1976) 31(14):1539–1546. doi:10.1097/01.brs.0000221994.61882.4a

26. Liang CZ, Li H, Tao YQ, Peng LH, Gao JQ, Wu JJ, Li FC, Hua JM, Chen QX (2013) Dual release of dexamethasone and transforming growth factor beta3 from polymeric microspheres for the stem cell matrix accumulation in a rat disc degeneration model. Acta Biomater. doi:10.1016/j.actbio.2013.08.019

27. Dominici M, Le Blanc K, Mueller I, Slaper-Cortenbach I, Marini F, Krause D, Deans R, Keating A, Prockop D, Horwitz E (2006) Minimal criteria for defining multipotent mesenchymal stromal cells. The International Society for Cellular Therapy position statement. Cytotherapy 8(4):315–317. doi:10.1080/14653240600855905

28. Boxall SA, Jones E (2012) Markers for characterization of bone marrow multipotential stromal cells. Stem Cells Int 2012:975871. doi:10.1155/2012/975871

29. Yoshimura H, Muneta T, Nimura A, Yokoyama A, Koga H, Sekiya I (2007) Comparison of rat mesenchymal stem cells derived from bone marrow, synovium, periosteum, adipose tissue, and muscle. Cell Tissue Res 327(3):449–462. doi:10.1007/s00441-006-0308-z

30. Hansen MB, Nielsen SE, Berg K (1989) Re-examination and further development of a precise and rapid dye method for measuring cell growth/cell kill. J Immunol Methods 119(2):203–210

31. Postacchini F, Bellocci M, Massobrio M (1984) Morphologic changes in annulus fibrosus during aging. An ultrastructural study in rats. Spine (Phila Pa 1976) 9(6):596–603

32. Sakaguchi Y, Sekiya I, Yagishita K, Muneta T (2005) Comparison of human stem cells derived from various mesenchymal tissues: superiority of synovium as a cell source. Arthritis Rheum 52(8):2521–2529. doi:10.1002/art.21212

33. Karaoz E, Aksoy A, Ayhan S, Sariboyaci AE, Kaymaz F, Kasap M (2009) Characterization of mesenchymal stem cells from rat bone marrow: ultrastructural properties, differentiation potential and immunophenotypic markers. Histochem Cell Biol 132(5):533–546. doi:10.1007/s00418-009-0629-6

34. Lotfy A, Salama M, Zahran F, Jones E, Badawy A, Sobh M (2014) Characterization of mesenchymal stem cells derived from rat bone marrow and adipose tissue: a comparative study. Int J Stem Cells 7(2):135–142. doi:10.15283/ijsc.2014.7.2.135

35. Barzilay R, Sadan O, Melamed E, Offen D (2009) Comparative characterization of bone marrow-derived mesenchymal stromal cells from four different rat strains. Cytotherapy 11(4):435–442. doi:10.1080/14653240902849796

36. Rebelatto CK, Aguiar AM, Moretao MP, Senegaglia AC, Hansen P, Barchiki F, Oliveira J, Martins J, Kuligovski C, Mansur F, Christofis A, Amaral VF, Brofman PS, Goldenberg S, Nakao LS, Correa A (2008) Dissimilar differentiation of mesenchymal stem cells from bone marrow, umbilical cord blood, and adipose tissue. Exp Biol Med (Maywood) 233(7):901–913. doi:10.3181/0712-RM-356

37. Zhu H, Mitsuhashi N, Klein A, Barsky LW, Weinberg K, Barr ML, Demetriou A, Wu GD (2006) The role of the hyaluronan receptor CD44 in mesenchymal stem cell migration in the extracellular matrix. Stem Cells 24(4):928–935. doi:10.1634/stemcells.2005-0186

38. Son BR, Marquez-Curtis LA, Kucia M, Wysoczynski M, Turner AR, Ratajczak J, Ratajczak MZ, Janowska-Wieczorek A (2006) Migration of bone marrow and cord blood mesenchymal stem cells in vitro is regulated by stromal-derived factor-1-CXCR4 and hepatocyte growth factor-c-met axes and involves matrix metalloproteinases. Stem Cells 24(5):1254–1264. doi:10.1634/stemcells.2005-0271

39. Xu X, Zhu F, Zhang M, Zeng D, Luo D, Liu G, Cui W, Wang S, Guo W, Xing W, Liang H, Li L, Fu X, Jiang J, Huang H (2013) Stromal cell-derived factor-1 enhances wound healing through recruiting bone marrow-derived mesenchymal stem cells to the wound area and promoting neovascularization. Cells Tissues Organs 197(2):103–113. doi:10.1159/000342921

40. Mayer H, Bertram H, Lindenmaier W, Korff T, Weber H, Weich H (2005) Vascular endothelial growth factor (VEGF-A) expression in human mesenchymal stem cells: autocrine and paracrine role on osteoblastic and endothelial differentiation. J Cell Biochem 95(4):827–839. doi:10.1002/jcb.20462

41. Reems JA, Torok-Storb B (1995) Cell cycle and functional differences between CD34$^+$/CD38hi and CD34$^+$/38lo human marrow cells after in vitro cytokine exposure. Blood 85(6):1480–1487

42. Jaenisch R, Young R (2008) Stem cells, the molecular circuitry of pluripotency and nuclear reprogramming. Cell 132(4):567–582. doi:10.1016/j.cell.2008.01.015

43. Carlin R, Davis D, Weiss M, Schultz B, Troyer D (2006) Expression of early transcription factors Oct-4, Sox-2 and Nanog by porcine umbilical cord (PUC) matrix cells. Reprod Biol Endocrinol 4:8. doi:10.1186/1477-7827-4-8

44. Izadpanah R, Joswig T, Tsien F, Dufour J, Kirijan JC, Bunnell BA (2005) Characterization of multipotent mesenchymal stem cells from the bone marrow of rhesus macaques. Stem Cells Dev 14(4):440–451. doi:10.1089/scd.2005.14.440

45. Silva J, Nichols J, Theunissen TW, Guo G, van Oosten AL, Barrandon O, Wray J, Yamanaka S, Chambers I, Smith A (2009) Nanog is the gateway to the pluripotent ground state. Cell 138(4):722–737. doi:10.1016/j.cell.2009.07.039

46. Boyle M, Wong C, Rocha M, Jones DL (2007) Decline in self-renewal factors contributes to aging of the stem cell niche in the drosophila testis. Cell Stem Cell 1(4):470–478. doi:10.1016/j.stem.2007.08.002

47. Carlson ME, Conboy IM (2007) Loss of stem cell regenerative capacity within aged niches. Aging Cell 6(3):371–382. doi:10.1111/j.1474-9726.2007.00286.x

48. Gopinath SD, Rando TA (2008) Stem cell review series: aging of the skeletal muscle stem cell niche. Aging Cell 7(4):590–598. doi:10.1111/j.1474-9726.2008.00399.x

49. Hunter CJ, Matyas JR, Duncan NA (2004) Cytomorphology of notochordal and chondrocytic cells from the nucleus pulposus: a species comparison. J Anat 205(5):357–362. doi:10.1111/j.0021-8782.2004.00352.x